PHYSICAL REVIEW B VOLUME 16, NUMBER 5 1 SEPTEMBER 1977

Spectral energy transfer in PrF_3, $PrCl_3$†

D. S. Hamilton,* P. M. Selzer, and W. M. Yen
Department of Physics, University of Wisconsin, Madison, Wisconsin 53706
(Received 27 April 1977)

Time-resolved fluorescence line narrowing is used to study spectral energy transfer in PrF_3 and $PrCl_3$. The excitation spectrum of PrF_3 in the region of the $({}^3H_4)_1 \rightarrow {}^3P_0$ absorption indicates that several strong satellite lines accompany the main transition, their origin being ascribed to different Pr^{3+} ions lying in strongly perturbed lattice sites. The spectral transfer within the inhomogeneously broadened main transiton is measured, where the energy mismatch is about 2 cm^{-1}. This process is characterized by a strong ($\sim T^{4.3}$) dependence of the transfer probability on sample temperature. The growth of the full inhomogeneous emission profile accompanies a uniform decay of the donor line shape. A transfer process between the lowest-energy satellite ions is also measured. Here the energy mismatch is 32 cm^{-1} resulting in a weak temperature dependence for the transfer rate. Both the intraline and intersatellite transfer are characterized by simple exponential rate equations. Recent calculations of phonon-assisted transfer probabilities are compared to our measurements, with the intersatellite transfer ascribed to a "one-phonon direct" process whereas the transfer within the main transition occurs by a "one-phonon second-order" mechanism. In $PrCl_3$ the transfer times are faster than the 15-nsec response time of our detection system indicating a much stronger ion-ion coupling.

I. INTRODUCTION

The static spectral properties of the fluorescence and absorption lines of rare-earth ions in crystals have been extensively studied with crystal-field and phonon relaxation theories having had great success in explaining the position, number, and widths of these spectral lines. Much experimental work has also been devoted to the dynamics of energy transfer between different species of ($3d$) and/or ($4f$) ions doped into the same host.[1] Detailed analysis of these experiments allows the indirect study of energy transfer between ions of the same species.

Energy transfer *within* an inhomogeneously broadened optical transition of a single species has recently been observed in several impurity-doped crystalline and amorphous hosts[2-8] using the technique of time-resolved fluorescence line narrowing. These time-resolved fluorescence spectra show directly the spectral transfer from the initial set of excited ions (donor system) to the ions comprising the full inhomogeneous distribution (acceptor system). The temperature dependence of the transfer probability has indicated the phonon-assisted nature of this process.

The optically active ions in stoichiometric crystals have been discussed by many authors using an excitonic description for the collective excitation of the electronic states. This concept of delocalized or collective excitation is useful when the perturbation energy caused by strains or defects in the crystal is much less than the ion-ion coupling. For a weakly coupled system with a large inhomogeneous linewidth, a localized or single-ion description is more appropriate. In this article we consider two such stoichiometric crystals, PrF_3 and $PrCl_3$.

We have measured the excitation spectrum of PrF_3 in the region of the $({}^3H_4)_1 \rightarrow {}^3P_0$ absorption which indicates several "satellite lines" accompanying the main transition. These lines presumably arise from Pr^{3+} ions situated in strongly perturbed lattice environments and suggest the inhomogeneous broadening mechanism active in this crystal. Our experiments have determined that inhomogeneous broadening is indeed responsible for the width of main absorption line, and time-resolved fluorescence studies have revealed a two-phonon-assisted spectral transfer[9] of a similar character to that observed in[3,4] $LaF_3:Pr^{3+}$. An energy-transfer process between the different satellite ions is also measured. Here the energy mismatch is large and a weak temperature dependence for the transfer rate indicates a one-phonon mechanism.[10,11]

We have correlated our results with recent microscopic theoretical descriptions[9-11] of phonon-assisted spectral transfer. The temperature and energy mismatch dependences of the transfer rate are used to identify the dominant ion-phonon coupling term responsible for the transfer process. Phonon phase terms are shown to be responsible for the increase in the intraline transfer temperature dependence over that in $LaF_3:Pr$. The observed exponential dynamics are shown to be consistent with a macroscopic description of energy transfer including back-transfer terms.

In view of our results in PrF_3, we have attempted to observe spectral energy transfer in $PrCl_3$. The

characteristic transfer times are faster than our 15-nsec instrumental response time indicating the probable excitonic nature of the electronic states in this crystal.

II. EXPERIMENTAL DETAILS

The PrF_3 crystal was provided by Optovac, Inc. and was of "high optical quality." Observation of the fluorescence filament under well-focused laser excitation indicated little internal scattering arising from macroscopic flaws. The $PrCl_3$ crystal was obtained from Johns Hopkins through R. Sarup. Careful crystal handling resulted in a minimum of surface deterioration due to its hygroscopic properties.

The crystal was excited with a high-resolution, pulsed, pressure-tunable dye laser[12] as indicated in Fig. 1. Lasing is achieved by pumping the dye with a Molectron UV-400 nitrogen laser having a peak power of approximately 200 kW at a 40-Hz repetition rate and a 10-nsec pulse width. Coumarin 102, diluted to a 10^{-2} mol/L concentration in high-purity ethanol is appropriate for exciting the $(^3H_4)_1 \rightarrow {}^3P_0$ absorption at 4778 Å in PrF_3. Inserting an intracavity etalon with a 3.6-mm spacer narrowed the laser spectral width from 1 cm^{-1} to 1.0 GHz and an intracavity Glan-Thompson prism was used to control the polarization of the beam.

The crystal was mounted in a variable temperature helium cryostat along with a carbon-glass resistance thermometer. A dc heater and electronic controller maintained a 0.05-K temperature stability. Careful thermal sinking minimized the uncertainty in the temperature measurements and no heating from the laser excitation was observed.

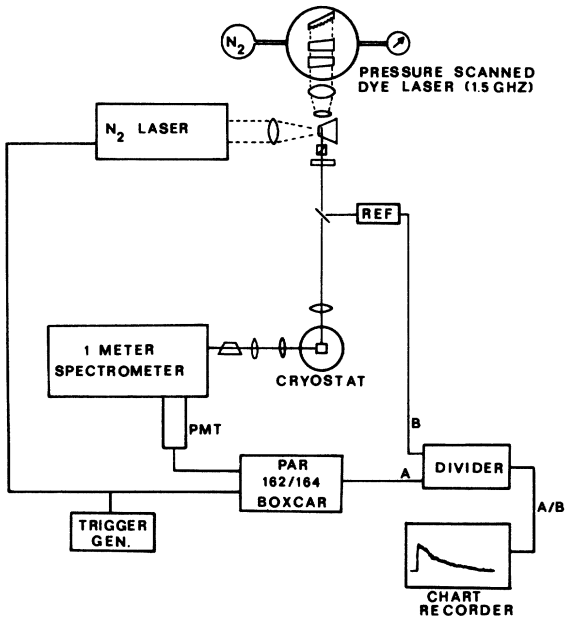

FIG. 1. Experimental arrangement for energy-transfer measurements, showing the dye laser in its higher-resolution mode.

The PrF_3 fluorescence was focused onto the entrance slit of a Spex 1-m spectrometer. When appropriate, the fluorescence was spatially rotated by placing a dove prism between the sample and the entrance slit. The 30-μm slit widths used throughout gave a 0.9-cm^{-1} resolution. An RCA 7265 photomultiplier tube with an S-20 cathode and a 7-nsec FWHM single-photon response time was used to detect the fluorescence. The high gain of this tube alleviated the need for additional signal amplification.

A PAR model 162/164 boxcar integrator measured the photomultiplier output with a 15-nsec gate width, and an external trigger generator provided the necessary synchronization between the laser pulse and the opening of the boxcar gate. Careful grounding and shielding reduced the rf pickup from the nitrogen laser to less than 1% of full scale. The boxcar output was then normalized to the dye-laser intensity, with the ratio displayed on an X-Y recorder. A total system response time of 15 nsec was measured for a 10%–90% rise in the fluorescence signal.

III. THEORETICAL REVIEW

The microscopic theory of energy transfer developed by Forster,[13] Dexter,[14] and Miyakawa[15] has been applied to many studies of energy transfer between different species of ions. More recent discussions[9-11,16-18] have been of a more fundamental nature in that they treat the ion-ion and ion-lattice interactions on equal footing. The temperature and energy mismatch dependences of the transfer probability arise in a natural way. We present here a synopsis of the relevant transfer probabilities calculated using perturbation theory.

The probability for the transfer of electronic excitation from ion 1 to ion 2 involving the emission or absorption of a single phonon of energy $E = \hbar\omega_{k,p}$ is[10,11]

$$W_{1\rightarrow 2} = \frac{2\pi}{\hbar^2} J^2 \sum_{\vec{k},p} \frac{\hbar}{2Mv_p^2} \frac{1}{\omega_{\vec{k},p}} [\Delta f^{(1)} - \Delta f^{(2)} e^{i\vec{k}_p \cdot \vec{R}_{12}}]^2 \times (n_{\vec{k},p} + \gamma)\, \delta(E_1 - E_2 - \hbar\omega_{\vec{k},p}) , \quad (1)$$

where J is the ion-ion (exchange, multipolar) coupling between ions 1 and 2, $\vec{R}_{1,2}$ is their spatial separation, and γ is 1(0) for phonon emission (absorption). The quantity $\Delta f^{(j)}$ is the difference in the ion-lattice coupling between the initial and final electronic states for ion j, i.e.,

$$\Delta f^{(j)} = \langle j^* | H_{ii}^{(j)} | j^* \rangle - \langle j | H_{ii}^{(j)} | j \rangle . \quad (2)$$

The temperature dependence for this process is

$$n_{k,\rho} + \gamma = 1/(e^{\hbar\omega/kT} - 1) + \gamma , \quad (3)$$

and indicates a strong energy mismatch asymmetry for $\Delta E \gtrsim kT$.

Recently, Holstein, Lyo, and Orbach[9] have calculated transfer probabilities for several higher-order phonon-assisted processes. Their "one-phonon second-order" process appears to dominate the spectral transfer within the main absorption line in PrF_3. For this mechanism the transfer rate is

$$W_{1\to 2} = \frac{2\pi}{\hbar} \sum_{\vec{k},\vec{k}'} J^2 \frac{(\Delta f)^4}{\hbar\omega_{\vec{k}}\,\omega_{\vec{k}'}} \langle n_{\vec{k}'} + 1 | \epsilon | n_{\vec{k}'} \rangle \times \langle n_{\vec{k}} - 1 | \epsilon | n_{\vec{k}} \rangle |^2 \langle h \rangle \times \delta(\hbar\omega_{\vec{k}'} - \hbar\omega_{\vec{k}} - \Delta E) , \quad (4)$$

where $\langle h \rangle$ is an angular average of a phonon-phase interference term

$$h(\vec{k},\vec{k}') = | e^{i\vec{k}\cdot\vec{R}_{12}} + e^{-i\vec{k}\cdot\vec{R}_{12}} - 1 - e^{i(\vec{k}-\vec{k}')\cdot\vec{R}_{12}} | . \quad (5)$$

For $kR \gg 1$ and $k'R \gg 1$, a T^3 temperature dependence is predicted with the rate being only weakly dependent on the energy mismatch ΔE for $\Delta E \lesssim kT$.

Other higher-order phonon-assisted processes are characterized by a strong (varying as $1/\Delta E^2$) dependence on the energy mismatch. For a small ΔE, one might have a rapid spatial migration of the excitation with little spectral transfer. The importance of such a process depends on the probability of finding an ion with a small enough ΔE within a suitable distance through which the ion-ion coupling can act.

The validity of the time-dependent perturbation approach used in these calculations must be carefully considered. The ion-lattice coupling (H_{ii}) is sufficiently weak for the well-shielded $4f$ electrons to use the pure electronic wave functions $|j\rangle$ and $|j^*\rangle$.[16] A second limitation involves the strength of the ion-ion coupling relative to the ion-lattice interaction. We require that the phonon-assisted transfer times be longer than the vibrational relaxation time of the ion in order for the transfer to be an incoherent process.[19] Without a dephasing mechanism such as phonon relaxation, one must instead consider a coherent description for energy transfer. It is this vibrational relaxation or dephasing rate which determines how rapidly the electronic wave functions lose coherence and result in a homogeneous or lifetime broadening of the optical lines observed at finite temperatures. The homogeneous width arising from phonon relaxation varies from an extrapolated value of 5×10^{-7} cm^{-1} at 6 K to 4×10^{-2} cm^{-1} at 20 K for the $(^3H_4)_1 \to {}^3P_0$ transition in LaF_3:Pr.[5,20] This corresponds to relaxation rates of 1×10^{-5} to 1×10^{-10} sec, respectively. We anticipate our measured transfer rates by saying that the criteria for an incoherent phonon-assisted process are generally met for PrF_3.

We have also considered the nature of J, the ion-ion coupling mechanism. Following Kushida[21] we have calculated[22] an electric dipole-dipole interaction strength of $J \cong 7\times10^{-2}$ cm^{-1} for two nearest-neighbor Pr^{3+} ions in LaF_3. The quadrupole coupling terms vanish due to the $|\Delta J| \leq 2$ selection rule. A magnetic dipole coupling requires $|\Delta S| = |\Delta L| = 0$ and hence also vanishes.

Exchange can also couple two nearby rare-earth ions. A direct exchange process involving the overlap of the $4f$ wave functions should be negligible due to their small radial extent. A more plausible mechanism involves the mixing of the $4f$ and $5d$ wave functions at the two ion sites, with a direct exchange occurring for the $5d$ wave functions.[23] Estimates of the interaction strength for such a process are difficult to undertake. There is also a superexchange[24] process in which the Pr ions interact through a mutual exchange coupling with intervening fluorine ions. The coupling strength varies with the number and type of paths connecting the ions.

There are other considerations[25] which enter into the already complicated description of the ion-ion coupling. The linear and nonlinear shielding of the $4f$ electrons by the outer-electron orbitals will serve to modify the range dependence of the the interaction. The role of the intervening ligands in producing induced moments, overlap, and bonding covalency is not properly understood and may influence the nature of the ion-ion coupling strength.

Radiative processes can also lead to energy transfer within an inhomogeneously broadened line. It has recently been demonstrated[26] that this radiative mechanism can be estimated by replacing the nonradiative ion-ion coupling J by $J' = \lambda A/2\pi Rc$, where λ is the transition wavelength, A is the radiative decay probability for the $^3P_0 \to (^3H_4)_1$ transition, and R is the ion-ion separation. Assuming that this decay probability is approximately $A = 0.3\times10^{-3}$ sec^{-1},[28] we estimate $J' = 1\times10^{-6}$ cm^{-1} as compared to a dipolar nonradiative $J = 7\times10^{-2}$ cm^{-1}. Since it enters as J^2 in the transfer rate, we assume that radiative phonon-assisted transfer is negligible in our system.

The microscopic transfer rates can be related to the observed spectral dynamics by macroscopic rate equations. Consider the kth donor ion; initially excited at time $t = 0$, located at position $\vec{R}_k$ and having an excited-state energy of E_k. If $P_k(t)$

is the probability of finding this kth ion in its excited state at time t, then the time rate of $P_k(t)$ is

$$\frac{dP_k(t)}{dt} = - W_{st} P_k(t) - P_k(t) \sum_{j=1}^{N} W_{jk}(\vec{R}_{jk}, \Delta E_{jk}) + \sum_{j=1}^{N} P_j(t) W_{kj}(\vec{R}_{kj}, \Delta E_{kj}) . \quad (6)$$

The first term is the decay of ion k due to "single-ion" processes such as radiative or multiphonon deexcitation. Next is the term describing the probability for the transfer of excitation from ion k to its N neighbors each of which is located at $\vec{R}_j$, and the final term is involved with the transfer from the neighbors back to ion k. The solution to this equation depends on the environment of the donor ion and the form of the single-ion transfer probability $W_{jk}(\vec{R}_{jk}, \Delta E_{jk})$. One must then average over all the possible donor configurations to obtain the macroscopic behavior of the donor ensemble.

IV. EXCITATION SPECTRUM

The excitation spectrum of PrF_3 in the region of the $(^3H_4)_1 \rightarrow {}^3P_0$ absorption was measured at 6 K and is shown in Fig. 2. In order to obtain a signal proportional to the fraction of ions that absorb at a particular wavelength, the excitation volume sampled must have a thickness much less than the absorption length. Using a 1.0-GHz excitation source, the shortest absorption length is about 100 μm.[22] By magnification of the fluorescent image onto the narrow spectrometer slits, the first 3 μm of the excitation volume was observed. The spectrometer was placed in zeroth order and the fluorescence intensity was plotted as the dye laser was spectrally scanned.

The prominent feature in the excitation spectrum is at 4778 Å which we label A_0 and will refer to as line center or the main transition. Other strong lines are A_1 and A_2 at 20 and 18 cm^{-1} on the high-energy side of line center, respectively, and A_3 and A_4 at 30 and 62 cm^{-1} on the low-energy side. The width of A_0 is about 2.0 cm^{-1} FWHM and is comparable to the width of the rest of the features.

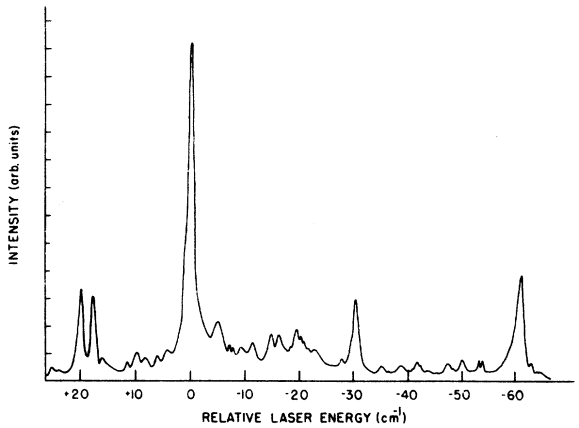

FIG. 2. Excitation spectra of PrF_3 in the region of the $(^3H_4)_1 \rightarrow {}^3P_0$ absorption.

The satellite lines ($A_1 \cdots A_4$ in Fig. 2) that accompany the main transition (A_0) are Pr^{3+} ions located in strongly perturbed lattice environments. Their identification as Pr^{3+} ions follows from the comparison of their fluorescence spectra to that of the A_0 ions and to those of Pr^{3+} ions in PrF_3 films[29] and in $LaF_3:Pr^{3+}$.[11] A strong crystal-field perturbation due to these ions being located at or near irregular lattice sites is presumably responsible for their energy states being shifted from the A_0 value. These irregular lattice sites are ascribed to vacancies, interstitial ions, impurities, or other lattice defects and have been observed in other crystals with high concentration of optically active ions.[30,31] We note that the high optical quality of the crystal probably rules out any large macroscopic defects. The satellite lines were also independent of the geometric position of the dye-laser excitation, again indicating the microscopic nature of the defects.

The existence of these lattice defects also points to the inhomogeneous nature of the main transition A_0. An ion located at a "normal" lattice site and having a nearby lattice irregularity will see a slightly distorted crystalline environment, hence will have its energy levels slightly shifted. The randomness in defect to normal site distance and orientation, thus leads to an inhomogeneous broadening of the ions at these locations.

V. MEASUREMENT OF ENERGY-TRANSFER RATES

A direct measurement of the probability for the transfer of excitation from ion 1 to ion 2 implicitly assumes a method exists for distinguishing between the two ions. The most experimentally accessible characteristic is their difference in excited-state energy. Thus, we will be concerned with investigating the transfer rate between ions 1 and 2 whose excited states are separated by an energy mismatch ΔE_{12}. This requirement limits the possible process for spectral-energy transfer to those having a frequency shifting mechanism, i.e., a phonon-assisted process.

We operationally define the donor system as that ensemble of ions excited at time $t = 0$ by the pulsed dye laser. The energy spread of this ensemble is the sum of the dye-laser width and the averaged homogeneous width of the ions. The population of this donor ensemble is monitored by observing

the fluorescence characteristic of these ions. As time evolves following the initial pulsed excitation, energy is transferred from the donor ensemble to the acceptor ensemble. We measure this process by observing the growth of the fluorescence characteristic of the acceptor population for times $t>0$. The transfer probability is extracted by monitoring the donor and acceptor fluorescence at different time delays after the laser pulse excitation.

A. Transfer within the main absorption line

We now present our measurements of the spectral energy transfer within the main $(^3H_4)_1 \rightarrow {}^3P_0$ transition; that is, the A_0 set of sites indicated by the excitation scan. The mere existence of line narrowing and the fact that the narrowed component tunes with the laser across the absorption profile, demonstrates the inhomogeneous character of this line. In order to excite a small fraction of Pr ions within this ~2-cm^{-1} linewidth, the dye laser was used in its intermediate resolution configuration where the spectral width is about 1.0 GHz (0.03 cm^{-1}). As mentioned previously, the resonant $^3P_0 \rightarrow (^3H_4)_1$ fluorescence for the A_0 ions is weak due to some reabsorption and a small branching ratio for this transition. We therefore used the much stronger but nonresonant $^3P_0 \rightarrow (^3H_6)_1$ fluorescence to monitor the population of the donor and acceptor ions despite the residual inhomogeneous broadening due to the accidental coincidence effect[5,32] for nonresonant transitions. This residual broadening does not complicate the direct observation of the energy-transfer process, and nonresonant transitions have been used to study similar processes in LaF_3 : Pr.[3-5]

Time-resolved emission spectra showing the intraline spectral-energy transfer in PrF_3 are illustrated in Fig. 3. Here the laser is pumping those ions whose absorption is 2 cm^{-1} on the high-energy side of line center. The growth of the acceptor population at the expense of the donors is clearly demonstrated by these spectra. At a 1-μsec delay, the donor population has almost vanished and the acceptor fluorescence begins to decay through other deexcitation channels.

These scans point out the spectral characteristics of the energy-transfer process. The profiles of the donor and acceptor fluorescence are seen to rise and fall uniformly. We observe no distinguishable broadening or other change in the line shape of the donor fluorescence with time. These characteristics are similar to those observed in the lower-concentration LaF_3:Pr^{3+} studies.[3-5]

The dynamics and temperature dependence for this process were measured by pumping at the edge of the absorption line and using the spectrometer to separate the donor from the acceptor line shape. That is, by fixing the spectrometer at the wavelength of the donor fluorescence and then scanning the delay of the boxcar integrator, the time evolution of the donor population is easily extracted. Similarly, we can monitor the acceptor population by moving the spectrometer to the acceptor fluorescence wavelength.[33]

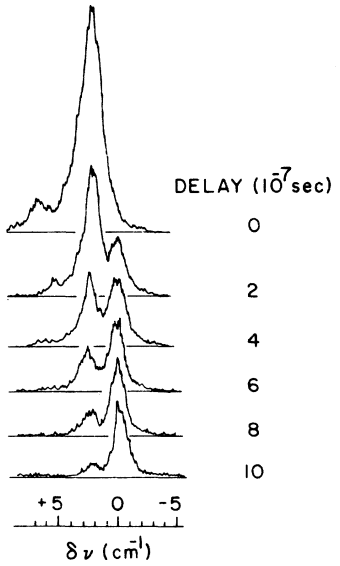

FIG. 3. Time resolved $^3P_0 \rightarrow (^3H_6)_1$ emission spectra of the A_0 ions.

The time development of the donor and acceptor ions is shown in Fig. 4, where we have scanned the boxcar gate while using the spectrometer to isolate the donor and acceptor fluorescence. The dye laser is now 4 cm^{-1} on the low-energy side of line center and the sample temperature is 15 K. The rise of the acceptor fluorescence intensity from a value of zero at $t=0$ is evidence that we have adequately spectrally isolated the donor and acceptor fluorescence.

In Figs. 5 and 6 we illustrate semilog graphs of the same donor and acceptor fluorescence as

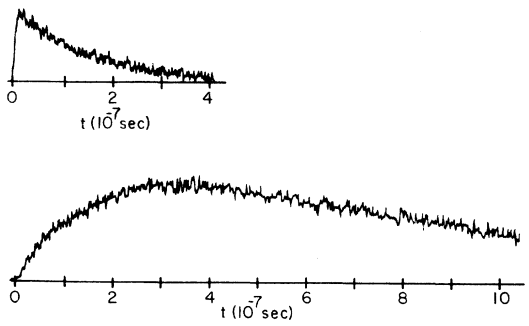

FIG. 4. Spectral dynamics of the A_0 donor and acceptor emission.

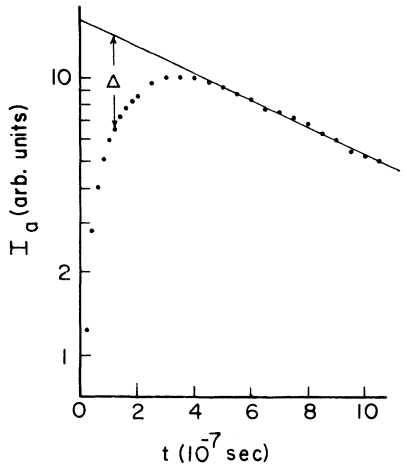

FIG. 5. Typical acceptor decay curve. The exponential tail of the fluorescence is used to extract $\Delta(t)$.

shown in Fig. 4. The transfer rates are calculated using simple rate equations for the donor and acceptor excited-state populations. The time evolution of these populations is assumed to be described by

$$\frac{dN_d}{dt} = -W_d N_d - W_{d\to a} N_d \tag{7}$$

and

$$\frac{dN_a}{dt} = +W_{d\to a} N_d - W_a N_a, \tag{8}$$

with the initial conditions $N_d(t=0) = N_0$ and $N_a(t=0) = 0$. Here $W_{d\to a}$ is the donor to acceptor spectral-transfer rate, and W_d and W_a are the rates for other decay channels for the donor and acceptor ions, respectively. The solution to these differential equations is easily shown to be

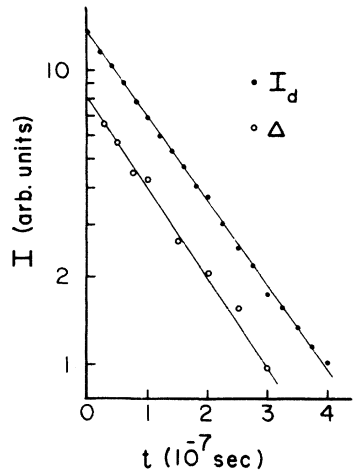

FIG. 6. Exponential dynamics of the donor emission compared to $\Delta(t)$, as obtained from Fig. 5.

$$N_d(t) = N_0 \exp[-(W_{d\to a} + W_d)t], \tag{9}$$

and

$$N_a(t) = \frac{N_0 W_{d\to a}}{W_{d\to a} + W_d - W_a}\left(e^{-W_a t} - e^{-(W_{d\to a}+W_d)t}\right) \tag{10}$$

A justification of this simple rate-equation description as well as the processes responsible for W_d and W_a is discussed in Sec. VI.

The tail of the acceptor fluorescence in Fig. 5 is fit to $W_a = 1.1\times10^6$ sec^{-1} and $\Delta(t)$ is then graphically evaluated as shown. In Fig. 6 a straight-line fit on this semilog graph of $\Delta(t)$ gives $W_{d\to a} + W_d = 6.8\times10^6$ sec^{-1} which agrees very nicely with the value extracted from the donor fluorescence of 6.6×10^6 sec^{-1}. In order to extract $W_{d\to a}$ we now assume that $W_d = W_a$ based on the fact that the donor and acceptor ions are in very similar environments and that their distances to traps or satellite ions as well as their ion-lattice coupling strengths are almost identical. The nearly-temperature-independent[34] value of $W_d = W_a = (1.1\pm0.2)\times10^6$ sec^{-1} is then subtracted from $W_{d\to a} + W_d$ to evaluate $W_{d\to a}(T, \Delta\tilde{\nu})$. For the data points discussed above, we have $W_{d\to a}(15\text{ K}, -4\text{ cm}^{-1}) = 5.7\times10^6$ sec^{-1}, with an estimate 0.5×10^6-sec^{-1} error arising from the combined uncertainties in $W_{d\to a} + W_d$ and W_a.

Using this analytic technique, we have conducted an evaluation of the donor to acceptor transfer rate in the 6–20 K temperature range. Data was taken with the laser pumping 2 cm^{-1} on the high-energy side of line center ($\Delta\tilde{\nu} = 2$ cm^{-1}) and 4 cm^{-1} on the low-energy side ($\Delta\tilde{\nu} = -4$ cm^{-1}). The temperature and energy mismatch dependence of this transfer rate are illustrated in Fig. 7. This figure indicates the strong relationship of the transfer probability on sample temperature. Also important is the weak dependence on the magnitude and sign of $\Delta\tilde{\nu}$, the rates for $\Delta\tilde{\nu} = 2$ cm^{-1} and $\Delta\tilde{\nu} = -4$ cm^{-1} being almost identical within the experimental

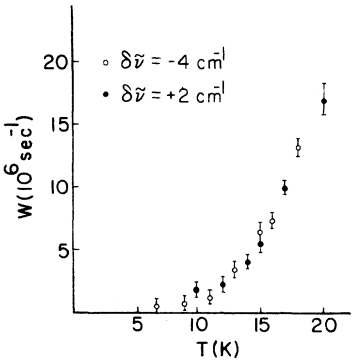

FIG. 7. Temperature dependence of the spectral-transfer rate among the A_0 ions.

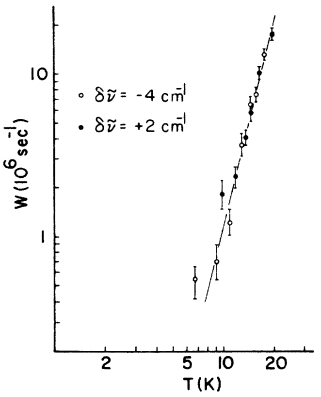

FIG. 8. Power-law fit to the $A_0 \rightarrow A_0$ spectral-transfer rate. The straight line indicates a $T^{4.3}$ relationship.

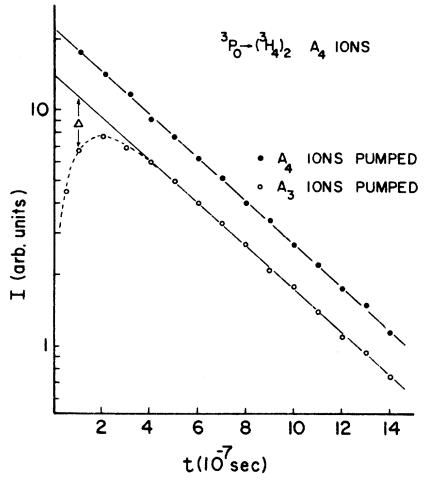

FIG. 9. Dynamics of the A_4 emission for excitation of the A_3 and A_4 ions.

error. These two facts are suggestive of the "one-phonon second-order" process. By plotting the results on log-log coordinates a power-law fit to the temperature dependence is obtained. The straight line in Fig. 8 indicates a relationship of

$$W_{a\rightarrow a}(T) \simeq (4.5 \pm 1.5) \times 10^1 \; T^{4.3 \pm 0.5} \; \text{sec}^{-1}.$$

B. Transfer among the satellite ions

The excitation spectra of PrF_3 indicates the presence of several strong satellite lines accompany the main $(^3H_4)_1 \rightarrow {}^3P_0$ transition. By selectively exciting one of the unique sets of satellite ions, we observe the dynamics of the energy transfer to other sets of satellite ions. Here, the dye laser was used with a 1-cm^{-1} spectral width since high resolution is not required.

The lowest-energy absorption is that of the A_4 ions at 4792.3 Å. With the dye laser tuned to this absorption, prominent fluorescence lines were observed at 4792.3, 4806.5, and 4811.0 Å ($T = 5.9$ K). The rise time of the fluorescence intensity is less than the 15-nsec instrumental response time. Because of this fast rise time and the close correlation with the expected wavelengths, these lines must then be components of the $^3P_0 \rightarrow (^3H_4)_n$ transitions of the A_4 ions.

The next-higher-energy absorption is that of the A_3 ions at 4785.0 Å. With the dye laser now tuned to this absorption, a new set of fluorescence lines are observed. These are at 4784.9, 4799.8, and 4804 Å. Again the lines have rise times of less than 15 nsec, and are clearly the $^3P_0 \rightarrow (^3H_4)_{1,2,3}$ transitions of the A_3 ions. In addition, as the A_3 ions are pumped the transitions of the A_4 ions are also observed, but now exhibit a markedly slower rise time. This rise time is characteristic of an energy-transfer process from the A_3 ions to the lower-energy A_4 ions.

The same rate equations are assumed for the intersatellite transfer as for the intraline transfer, with the donor and acceptor ions redefined as those comprising the A_3 and A_4 distributions, respectively. In Fig. 9 we illustrate the dynamics of the $A_3 \rightarrow A_4$ transfer process. The upper curve is the 4806.5 Å $^3P_0 \rightarrow (^3H_4)_2$ fluorescence of the A_4 ions after direct excitation and is exponential over more than one decade. The lower curve is the same fluorescence of the A_4 ions following laser excitation of the A_3 ions. The growth of this fluorescence is given by $\Delta(t)$ and we illustrate this $\Delta(t)$ along with the temporal decay of the A_3 donor fluorescence in Fig. 10. The applicability of the simple rate equations is demonstrated by the exponential behavior in both Figs. 9 and 10.

To investigate the role of phonons in this 32-cm^{-1} energy-transfer process from the A_3 sites to the

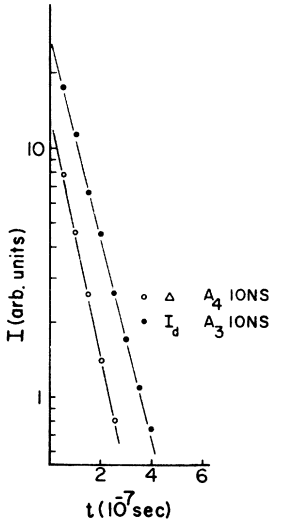

FIG. 10. Decay of the A_3 donor emission as compared to $\Delta(t)$ derived from the A_4 acceptor fluorescence.

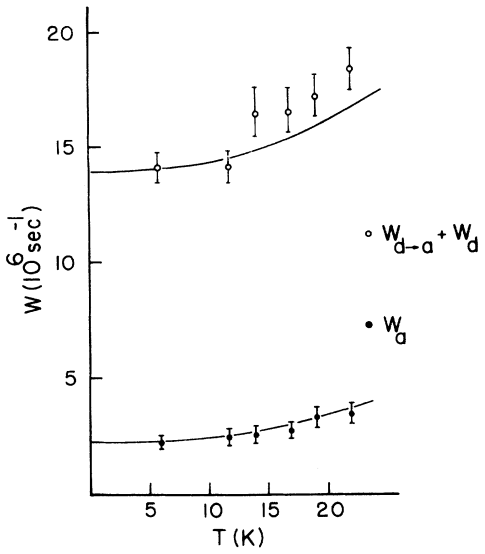

FIG. 11. Temperature dependence of the $A_3 \rightarrow A_4$ transfer process. The straight lines indicate $[\exp(\Delta\tilde{\nu}/0.77)-1]^{-1}$, where $\Delta\tilde{\nu}=32$ cm^{-1} for $W_{d\rightarrow a}+W_d$ and 22 cm^{-1} for W_a.

A_4 sites, we have analyzed the dynamics of the 4806.5-Å acceptor fluorescence at several different temperatures. The temperature dependence of the extracted rates is illustrated in Fig. 11. This weak temperature dependence and the fact that the energy mismatch between the A_3 and A_4 ions is 32 cm^{-1}, lead us to postulate that the responsible mechanism is the "one-phonon direct" process.[9-11] Finally, in regard to the $A_3 \rightarrow A_4$ transfer, we note that in the temperature range studied, no $A_4 \rightarrow A_3$ transfer was observed since such a process would require the absorption of a 32-cm^{-1} phonon.

We now turn to the other sets of ions observed in the excitation spectra. When the line center or A_0 sites are directly excited, the observed fluorescent lines increase in number. Qualitatively, the $A_0 \rightarrow A_3$ and $A_0 \rightarrow A_4$ transfer processes can be identified although their rates are much slower than the $A_3 \rightarrow A_4$ rate as indicated by the weak intensity of the A_3 and A_4 fluorescence. The large number of lines observed and their finite widths [especially the strong A_0 fluorescence to the $(^3H_4)_2$ and $(^3H_4)_3$ states] makes spectral isolation of the $A_0 \rightarrow A_3$ and $A_0 \rightarrow A_4$ transitions impractical.

The fluorescence spectrum when the A_1 and A_2 ions are directly pumped with the dye laser has also been observed. Their coupling to the A_3 and A_4 sites is strong as evidenced by the intensity of the A_3 and A_4 fluorescence with only a very weak A_0 fluorescence. At 6 K we measure a rate for $W_d + W_{d\rightarrow a}$ of 7.3×10^6 sec^{-1} for the A_1 sites and 6.7×10^6 sec^{-1} for the A_2 sites. No detailed temperature dependence was taken, but qualitatively the deexcitation rate for these ions is again only weakly temperature dependent.

C. Transfer in $PrCl_3$

We have also considered energy transfer in the $PrCl_3$ lattice. Here the Pr^{3+} ion sees a C_{3h} site symmetry, and hence, not all the $2J+1$ degeneracy is removed by the static crystal field. The ground state is now a doublet (twofold degenerate) as opposed to PrF_3 where all of the states are singlets.

The experimental techniques are similar to those used in the PrF_3 investigation. Much of the work was done however in a liquid-helium immersion Dewar where the sample temperature was about 2 K. The tendency of $PrCl_3$ to lase was minimized by defocusing the incident laser beam. Using either a 1-m grating spectrometer or a pressure-scanned high-resolution Fabry-Perot interferometer, the fluorescence lines originating from the $^3P_0(\mu=0)$ and terminating on the $^3H_6(\mu=3)$, $^3H_6(\mu=2)$, or the $^3F_2(\mu=2)$ were observed.

The measured linewidths for these various transitions were in essential agreement with those of German and Kiel,[35] with transitions terminating on doublets significantly broader than the singlet lines. These authors have attributed the doublet widths to fluctuations modulating the doublet splitting far above the ordering temperature of ~0.4 K.[36]

The important characteristic of the fluorescence transitions for our energy-transfer studies was the observation that the spectral location of the fluorescence did not change when the wavelength of the dye laser was shifted, nor were any spectral dynamics observed. We interpret our results as indicating that the transfer between Pr ions in this crystal is much faster than the 15-nsec response time of our detection system. This measurement allows us to put an upper limit on the single-ion to single-ion transfer time of about $\tau \lesssim 5\times10^{-8}$ sec at 2 K. This is almost three orders of magnitude faster than the extrapolated value for PrF_3 at 2 K for transfer within the main A_0 distribution.

VI. DISCUSSION

The spectral transfer within the inhomogeneously broadened A_0 ion distribution was experimentally characterized by a $T^{4.3}$ temperature-dependent and energy-mismatch-independent transfer rate. Also important was the uniform rise of the full inhomogeneous emission profile with the dynamics described by simple rate equations. Before treating these observations, we first discuss the processes responsible for W_a and W_d.

In order to separate the transfer rate $W_{d\to a}$ from the measured values of $W_{d\to a}+W_d$ we have assumed $W_d=W_a$ for the intraline transfer. In very low concentration systems, W_d and W_a represent radiative decay rates that are nearly constant across a reasonably narrow inhomogeneous line. Although this radiative decay rate may be somewhat higher in PrF_3 than the 2×10^4-sec^{-1} rate measured[27,28] for LaF_3:Pr it is probably too low to account for either W_a or W_d. A two-ion cross-relaxation process to the $^1G_4$ manifold has been discussed by Brown *et al.*[27] as a relaxation channel for the $^3P_0$ state in LaF_3:Pr and such multi-ion transitions may be a dominant deexcitation process in concentrated Pr^{3+} systems.[37] Using the PrF_3 energy levels,[10] a two-ion transition of the form $^3P_0$; $(^3H_4)_1\to(^1G_4)_9$; $(^1G_4)_8$ requires the emission of a 160-cm^{-1} phonon, and hence should be nearly temperature independent in the temperature region studied. A transfer to the A_3 and A_4 ions can also serve to depopulate the A_0 distribution. Again, this process should have a weak temperature dependence due to the large (30 and 62 cm^{-1}) energy mismatches. In addition, since the A_3 and A_4 acceptor emission is very weak upon excitation of the A_0 ions, a slow rate for this process is expected. Although our measurements do not establish the exact nature of the intrinsic donor and acceptor decay, their similar crystalline fields and energy levels support our assumption that $W_d=W_a$ for the intraline transfer process.

The dynamics for the intraline transfer were well described by simple exponential rate equations. From Eq. (6), the decay of the kth donor ion is a solution to

$$\frac{dP_k(t)}{dt}=-P_k(t)\sum_j W_{kj}-P_k(t)\sum_n W'_{kn}+\sum_j P_j(t)W_{jk}\,, \tag{11}$$

where W_{kj} and W_{jk} are the incoherent spatial transfer and back-transfer rates and W'_{kn} is the two-ion cross-relaxation rate. For PrF_3, where every ion site is occupied by a Pr^{3+} ion, it is the back-flow term that will lead to a nonexponential solution and not the donor configurational averaging. It can be shown[38] that by including the back transfer from the first set of nearest-neighbor acceptors, an approximate solution at short delays to Eq. (11) is

$$P_k(t)=\exp\left(\sum_n -W'_{kn}t\right)\times\exp\left(\sum_j -W_{kj}t+\ln(\cosh W_{kj}t)\right). \tag{12}$$

Using the lattice structure of PrF_3 and assuming that $W_{kj}=W_0(R_0/R_{kj})^6$ and $W'_{kn}=W'_0(R_0/R_{kn})^6$, where R_0 is the nearest-neighbor separation and W_0, W'_0 are chosen to model our measured decay probability, our computer computations indicate that Eq. (12) does not significantly deviate from an exponential over the first 1.5 decades. We feel these results model well the observed exponential transfer dynamics, and thereby justify their description by simple rate equations [Eqs. (7) and (8)].

The spectral characteristics of the transfer within the A_0 distribution are described by the uniform decay of the donor-emission profile and a uniform growth of the full A_0 inhomogeneous line shape. This observation is consistent with the weak dependence of the "one-phonon second-order" process on the energy mismatch. Also important is the energy distribution of acceptors around the initially excited donor ion. Our spectral observations are explained by assuming that the average donor ion is surrounded by an ensemble of acceptors, the majority of whose energy states span the full inhomogeneous line shape.

The origin of the inhomogeneous broadening of the A_0 ions is the presence of lattice defect centers mentioned previously. Ions closest to the defect centers are presumably the strongly perturbed satellite ions. Ions slightly further out may lie in the broad background observed in the excitation scan. Going out a few more lattice spacings away from the defect center, the ions belonging to A_0 distribution are encountered. The energy of the jth A_0 ion can be written as

$$E_j=E_j^0+\sum_n\langle\phi_j|V(\vec{R}_n-\vec{R}_j)|\phi_j\rangle\,, \tag{13}$$

where E_j^0 is the energy without the perturbing defect center at $\vec{R}_n$ and $V(\vec{R}_n-\vec{R}_j)$ is the perturbation potential due to the defect center. For a sufficiently long-range potential (~ 5 lattice spacings) coupled with a defect concentration of a few percent, the values of E_j should show a high degree of randomness. This random energy distribution is consistent with our observed spectral characteristics for the intraline transfer.

Accompanying the spectral transfer, a spatial-transfer process which does not shift frequency and would remain undetected by our methods, may also be present. This could be an incoherent phonon-assisted or coherent resonant process. In a situation where the acceptor ions are randomized in energy, a phonon-assisted process varying as the inverse square of the energy mismatch has been shown to produce a temporal evolution of the emission lineshape.[39,40] In a less-random configuration, however, such a process could produce a rapid spatial migration with little spectral transfer. A coherent resonant process may also lead to a rapid spatial migration between nearby ions nearly matched in

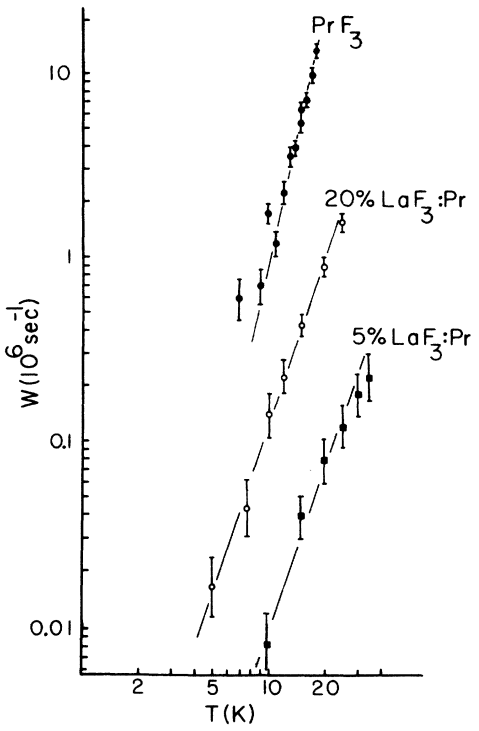

FIG. 12. Comparison of the spectral-transfer rates within the inhomogeneous $^3P_0$ state for PrF_3, 20% LaF_3:Pr, and 5% LaF_3:Pr.

energy. Recent energy-transfer measurements in dilute ruby[7,8] appear to show that a coherent spatial diffusion coexists with the slower spectral transfer, suggesting a less-than-random distribution in energy. Since there is no evidence at present to support the existence of spatial transfer as distinct from the observed spectral transfer in PrF_3, we shall ignore these effects and assume that a microscopic randomness occurs in this system.

In Fig. 12 we illustrate the temperature dependence of the intraline transfer in PrF_3 along with those for 5% LaF_3:Pr^{3+} (Ref. 3) and 20% LaF_3:Pr^{3+} (Refs. 4 and 41) which are shown with a fit to a T^3 dependence. The somewhat steeper relationship for the PrF_3 curve arises from the phonon-phase terms $\langle h \rangle$ of Eqs. (4) and (5). For a fixed value of k and k', as the ion-ion separation decreases the temperature dependence changes from T^3 for kR and $k'R \gg 2\pi$ to a T^7 relationship when kR and $k'R \lesssim \frac{1}{2}\pi$.[42] We have completed a more detailed calculation of the temperature dependence for this process by integrating Eq. (4) using a Debye phonon spectrum. The results[22] indicate a nearly $T^{6.1}$ dependence for PrF_3 as compared to the measured $T^{4.3}$ relationship. The calculated temperature dependence is very sensitive to the detailed nature of the phonon spectrum which may explain this discrepancy. We feel that the T^3 relationship for the 5% and 20% LaF_3:Pr^{3+} and the slightly steeper $T^{4.3}$ fit to the PrF_3 results demonstrate the role of the phonon-phase terms in the "one-phonon second-order" transfer process.

The intersatellite transfer between the A_3 and A_4 ions was experimentally characterized by a weak dependence of $W_{d\to a} + W_d$ on sample temperature and again, simple rate equations for the temporal evolution of the donor and acceptor emission. For this problem, however, the separation of the transfer rate from $W_{d\to a} + W_d$ is more difficult than for the intraline transfer since the acceptor decay rate now shows a measureable temperature dependence. Due to the shifted energy levels the energy mismatch may be altered from the line-center values, causing a different temperature dependence of the A_3 and A_4 ions for a cross-relaxation process. Nearby lattice defects may also serve to quench the donor and acceptor emission. The dissimilar lattice environments of the A_3 and A_4 ions is further reason for not allowing us to assume $W_a = W_d$. Although the temperature dependence of W_a and W_d might not be identical, it is clear from Fig. 11 that if they are roughly the same, subtracting a slowly rising form for $W_d \simeq W_a$ from $W_{d\to a} + W_d$ should put $W_{d\to a}$ on a curve similar to that expected for a one-phonon direct process involving a 32-cm^{-1} energy mismatch.

We have also pumped into the wing of the A_3 satellite ion absorption to measure the spectral transfer among the A_3 ions. No transfer to the center of the A_3 emission profile was observed and an upper limit of 0.5×10^6 sec^{-1} was placed on the $A_3 \to A_3$ transfer rate compare to the $A_3 \to A_4$ rate of approximately 10×10^6 sec^{-1} and the $A_0 \to A_0$ rate of 2×10^6 sec^{-1} at 10 K. This suggests that the spatial separation between the A_3 ions is larger than the $A_3 - A_4$ or $A_0 - A_0$ separation.

These results are consistent with a model where the different satellite lines arise from Pr^{3+} ions located at different distances or orientations from the same impurity, interstitial, or vacancy detect. This model is similar to that used by Green *et al.*[43] in MnF_2, where a one-to-one correspondence can be established between the distance of a Mn ion from an impurity and its energy levels. We can also use this model to explain the exponential transfer dynamics between the A_3 and A_4 ions. The probability of finding the kth A_3 donor ion excited at time t can be found from

$$\frac{dP_k(t)}{dt} = -P_k(t)\sum_j W_{kj} - P_k(t)\sum_n W'_{kn}, \qquad (14)$$

where we have neglected the slow single-ion decay rate. Here, W_{kj} is the $A_3 \to A_4$ transfer rate, W'_{kn} is the two-ion cross-relaxation rate and we have set

the $A_4 \rightarrow A_3$ back-transfer rate to zero. The solution is simply

$$P_k(t) = \exp - \left(\sum_j W_{kj} + \sum_n W'_{kn} \right) . \quad (15)$$

We must now average over all the A_3 donor environments. Assuming a fixed $A_3 - A_4$ separation and noting that all A_3 ions are uniformly surrounded by other Pr^{3+} ion to which they can cross relax, then the configurational average of Eq. (15) becomes

$$\langle P_k(t) \rangle = \left\langle \exp - \left(\sum_j W_{kj} + \sum_n W'_{kn} \right) \right\rangle$$

$$= \exp - \left(W_{d \rightarrow a} + W_d \right) , \quad (16)$$

which is the form of our simple rate equations for the donor (A_3) fluorescence .

Using the weak temperature dependence of the $A_3 \rightarrow A_4$ transfer rate and its large (32 cm^{-1}) energy mismatch, we have identified the dominant transfer mechanism as the one-phonon direct process. A calculation of the magnitude transfer rate using Eq. (1) is most difficult due to a lack of knowledge about the relevant ion-lattice matrix elements. Making a long-wavelength approximation ($kR \ll 2\pi$) and assuming $(\Delta f^{(1)} - \Delta f^{(2)})^2 \simeq f^2 = 1 \times 10^5$ cm^{-2} and a dipolar coupling strength of $J \simeq 7 \times 10^{-2}$ cm^{-1} our estimate[22] for the transfer probability is over an order of magnitude slower than the measured rate. This comparison must be viewed in light of the necessarily crude assumptions needed to complete the calculation.

Our results in $PrCl_3$ indicate a very rapid transfer process in this system. Our lower limit of $W \gtrsim 2 \times 10^7$ sec^{-1} at 2 K compares with the values of 10^7 sec^{-1} deduced by Krautsky and Moos[44] and the faster 7×10^9 sec^{-1} extrapolated by Gandrud and Moos.[45] The similar ion-lattice coupling for PrF_3 and $PrCl_3$ suggests a much larger ion-ion interaction strength in the latter system.[35,36] For this situation, an excitonic description of the optically active ions may be more appropriate.

At present we are unable to determine whether the width of the singlet $^3P_0 \rightarrow {}^3H_6(\mu = 3)$ transition, 0.5 cm^{-1}, arises mainly from residual inhomogeneous broadening or reflects a true exciton bandwidth. If the latter were solely responsible a dispersion of 0.5 cm^{-1} this would indicate a coherent interion transfer rate of $\sim 10^{10}$ sec^{-1} assuming six nearest neighbors. This is certainly consistent with the larger of the above estimates. However, since the presence of defects and other rare-earth impurities are likely to contribute to a residual width also of this order, it is likely that there is both an inhomogeneous and a dispersive component to the linewidth. Their relative magnitudes must await further experimentation with lower-concentration samples.

ACKNOWLEDGMENTS

We would like to thank Professor David L. Huber for his continued interest in this work and numerous contributions. It is with pleasure that we acknowledge the involvement of Professor Raymond Orback. Our thanks to R. Sarup for the loan of several $PrCl_3$ samples and to R. Flach for his initial involvement with our energy-transfer experiments.

*Present address: Dept. of Physics, University of Southern California, Los Angeles, Calif. 90007.

†Work supported by the NSF under Grant No. DMR-73-02478.

[1]For a recent review in both crystal and amorphous, see, R. Riesfeld, Struct. Bonding 30, 65 (1976).
[2]N. Montegi and S. Shionoya, J. Lumin. 8, 1 (1973).
[3]R. Flach, D. S. Hamilton, P. M. Selzer, and W. M. Yen, Phys. Rev. Lett. 35, 1034 (1975).
[4]P. M. Selzer, D. S. Hamilton, R. Flach, and W. M. Yen, J. Lumin. 12/13, 737 (1976).
[5]R. Flach, D. S. Hamilton, P. M. Selzer, and W. M. Yen, Phys. Rev. B 15, 1248 (1977).
[6]M. J. Weber, J. Paisner, S. S. Sussman, W. M. Yen, L. A. Riseburg, and C. B. Brecher, J. Lumin. 12/13, 729 (1976).
[7]P. M. Selzer, D. S. Hamilton, and W. M. Yen, Phys. Rev. Lett. 38, 858 (1977).
[8]P. M. Selzer and W. M. Yen (unpublished).
[9]T. Holstein, S. K. Lyo, and R. Orbach, Phys. Rev. Lett. 36, 891 (1976).
[10]R. Orbach, in *Optical Properties of Ions in Crystals*, edited by H. M. Crosswhite and H. W. Moos (Interscience, New York, 1967), p. 445.
[11]R. J. Birgeneau, J. Chem. Phys. 50, 4282 (1969).
[12]R. Flach, I. S. Shahin, and W. M. Yen, Appl. Opt. 13, 2095 (1974).
[13]T. Forster, Ann. Phys. 2, 55 (1968).
[14]D. L. Dexter, J. Chem. Phys. 21, 836 (1953); Phys. Rev. 126, 1962 (1962).
[15]T. Miyakawa and D. L. Dexter, Phys. Rev. B 1, 2961 (1970).
[16]R. Orbach, in *Optical Properties of Ions in Solids*, edited by B. DiBartoli (Plenum, New York, 1975), p. 355.
[17]T. F. Soules and C. B. Duke, Phys. Rev. B 3, 262 (1971).
[18]M. Kohli and N. L. Huang Liu, Phys. Rev. B 9, 1008 (1974).
[19]D. L. Dexter, T. Forster, and R. S. Knox, Phys. Status Solidi 34, K159 (1969).
[20]W. M. Yen, W. C. Scott, and A. L. Schawlow, Phys.

Rev. 136, 271 (1964).
[21]T. Kushida, J. Phys. Soc. Jpn. 34, 1318 (1973).
[22]D. S. Hamilton, Ph.D. thesis (University of Wisconsin-Madison, 1976) (unpublished).
[23]H. G. Danielmeyer, Adv. Solid State Phys. 15, 253 (1975).
[24]R. J. Birgeneau, Appl. Phys. Lett. 13, 193 (1968).
[25]W. P. Wolf and R. J. Birgeneau, Phys. Rev. 166, 376 (1968).
[26]T. Holstein, S. K. Lyo, and R. Orbach, Phys. Rev. B (to be published).
[27]M. R. Brown, J. S. S. Whiting, and W. A. Shand, J. Chem. Phys. 43, 1 (1965).
[28]M. J. Weber, J. Chem. Phys. 48, 4774 (1968).
[29]S. V. Sayre and S. Freed, J. Chem. Phys. 23, 2066 (1955).
[30]G. A. Prinz and E. Cohen, Phys. Rev. 165, 335 (1968).
[31]I. N. Douglas, Phys. Status Solidi 648, 327 (1971).
[32]D. S. Hamilton, P. M. Selzer, D. L. Huber, and W. M. Yen, Phys. Rev. 14, 2183 (1976).
[33]Using the spectrometer to deconvolute the donor and acceptor emission requires the excitation be far enough into the wing of the line where the acceptor concentration is minimal.
[34]The 15-K value of W_a was measured as $(1.3 \pm 0.2) \times 10^6$ sec^{-1}.
[35]K. R. German and A. Kiel, Phys. Rev. Lett. 33, 1039 (1974).
[36]J. P. Harrison, Jan P. Hessler, and D. R. Taylor, Phys. Rev. B 14, 2979 (1976).
[37]K. R. German, A. Kiel, and G. Guggenheim, Phys. Rev. B 11, 2436 (1975).
[38]D. L. Huber, D. S. Hamilton, and B. Barnett (unpublished).
[39]T. Holstein, S. K. Lyo, and R. Orbach, Phys. Rev. B 15, 4693 (1977).
[40]T. Holstein, S. K. Lyo, and R. Orbach, in *Proceedings of the CNRS International Colloquium* (CRNS, Paris, 1977), p. 185.
[41]The 20% curve is an average of the points measured in Ref. 4.
[42]Also, for $\frac{1}{2}kR$ or $\frac{1}{2}k'R \lesssim \pi$, an additional spatial dependence for the transfer rate arises from these phase terms.
[43]R. L. Greene, D. D. Sell, R. S. Fergeson, G. F. Imbusch, and H. J. Guggenheim, Phys. Rev. 171, 600 (1968).
[44]N. Krautsky and H. W. Moos, Phys. Rev. B 8, 1010 (1973).
[45]W. B. Grandrud and H. W. Moos, J. Chem. Phys. 49, 2170 (1968).